Heat treatment of commercial Polydimethylsiloxane PDMS precursors:

Part I. Towards conversion of patternable soft gels into hard ceramics

Srisaran Venkatachalam[a, 1], Djamila Hourlier[a]*

[a] IEMN (CNRS, UMR 8520), Université Lille 1, Avenue Poincaré, CS60069, F-59652 Villeneuve d'Ascq Cedex, France.

* Corresponding author, e-mail: djamila.hourlier@iemn.univ-lille1.fr,

Tel.: +33 320197836, Fax: +33 320197884

Abstract

The commercially available polydimethylsiloxane (Sylgard®184) is a commonly known material in microelectronic and microfluidic industries as flexible substrates, device packing elements, lab-on-a-chip, or stamps. Recently, PDMS derived materials have attracted much interest in the development of broadband electromagnetic absorbers in the terahertz and microwave regions. When exposed to high temperature (T > 900 °C) PDMS undergoes profound transformations leading to derived solid nanocomposites made of graphitic phase embedded into silicon oxycarbide structure.

In this work, we discuss the PDMS thermal changes that have been evaluated using different analytical techniques (thermogravimetry-coupled mass spectrometry, and Raman spectroscopy). The pyrolysis of cross-linked gels in an inert atmosphere gave 50.94 wt% of solid residue at 1500 °C. It was observed that the presence of Si-H bonds in the curing agent promotes cross-linking between the siloxane backbones containing vinyl groups (Si-C_2H_3) through hydrosilylation reaction. However, excessive addition of curing agent impedes ceramic yield down to 20%. Above 1000 °C, Raman spectra show the formation of disordered sp^2 carbon that subsequently organizes with

[1] Present address : Bannari Amman Institute of Technology, Sathyamangalam, Tamil Nadu, India

the heat-treatment temperature. These carbon-rich silicon oxycarbide materials are remarkably resistance to oxidation even at 1500 °C.

Keywords: *polydimethylsiloxane, polymer-derived ceramics, pyrolysis, thermal stability, thermal oxidation*

1. Introduction

Since Yajima's pioneering work on silicon oxycarbide (SiC_xO_y) ceramic fibers in the seventies [1–3], the research has been bolstered by considerable efforts to investigate new methods of synthesis from various hybrid organic-inorganic polymers, in order to obtain new phases that produce materials with enhanced properties (e.g. chemical and thermal stability) when compared with the conventional methods. Silicon-based polymeric precursors have become by far the most studied and used starting polymers for ceramic materials. At the time, these polymers, though known since 1901 [4,5], presented a refreshing new approach to the preparation of new materials. Emphasis was on the synthesis and thermal conversion of precursors for preparation of materials usable at high temperatures. Less attention was given to their other physical properties.

Over the past two decades, however, research has been redirected towards new applications as fibers [6], batteries [7,8] and ceramic matrix composites [9,10] in addition to the thermostructural. Besides mechanical properties [11], thermal/thermo-oxidative stability [12], silicon oxycarbide based materials have other properties such as electrochemical activity [13], giant piezoresistivity [14], white light emissivity [15,16] and efficient electromagnetic wave absorption in the microwave [17], and recently, terahertz domain [18]. This kind of materials is readily obtained by pyrolysis of silicon-based polymers with hybrid organic-inorganic molecular networks that contain Si, H, C, and O [19]. One of the advantages of using polymers as starting precursors is that the

chemical composition in the residue can be easily modified by changing the nature of functional groups present in the initial molecular structure and/or the gaseous atmosphere and temperature during heat treatment [20]. For instance, pyrolysis of phenyltriethoxysilane (C_6H_5-Si-$(OC_2H_5)_3$) allows for the incorporation of up to 45 wt.% of free carbon in the SiC_xO_y ceramic matrices, whereas the (CH_3-Si-$(OC_2H_5)_3$) methyltriethoxysilane leaves only 9 wt.% of free carbon at the same temperature of heat treatment 1000 °C [21].

The functional side groups, such as hydrogen, aliphatic or aromatic units, attached to silicon do not only control the carbon content in the derived ceramic material but also influence the electronic, optical, and rheological properties of the polymer [22]. This last property is of considerable practical importance in the fabrication of complex shapes, such as, for example, the micrometer-sized ceramic structures that are useful in potential applications as terahertz microbolometers [23], micro-electromechanical devices [24–26], and hydrophobic surfaces [27]. For terahertz applications in particular, one of the requirements imposed on polymeric precursors is, not only their ability to form various geometrical shapes with dimensional accuracy ranging from micrometers to centimeters, but also their ability to produce near-net shaped components after pyrolysis. To date, micro-sized ceramic components have been achieved by casting a flexible polymer on a rigid mold or vice versa [24–26]. One of the most commonly used silicon-based polymers is Sylgard®184 polydimethylsiloxane (PDMS) elastomer. PDMS is commercially available and used in a variety of applications such as micro and nano-fluidic channels for lab-on-chip applications [28], biocompatible materials [29], and electrically insulating materials [30]. It is noteworthy that, for such applications the organosilicon (PDMS) gel is used as it is, not thermally converted into a ceramic material. The gels can be prepared as follows: the elastomer kit

contains two parts, namely the base (part A) and curing agent (part B). The base contains a linear chain of siloxane with dimethyl groups and with Si-vinyl end groups (0.68 mol %) [30], and a Pt catalyst complex [31]. The curing agent is rich in Si-H bonds [30] and may also contains other oligomers such as tetramethyl tetravinyl cyclotetrasiloxane [32]. Mixing these two parts results in a soft and flexible elastomer with the tentative molecular structure shown in Figure 1.

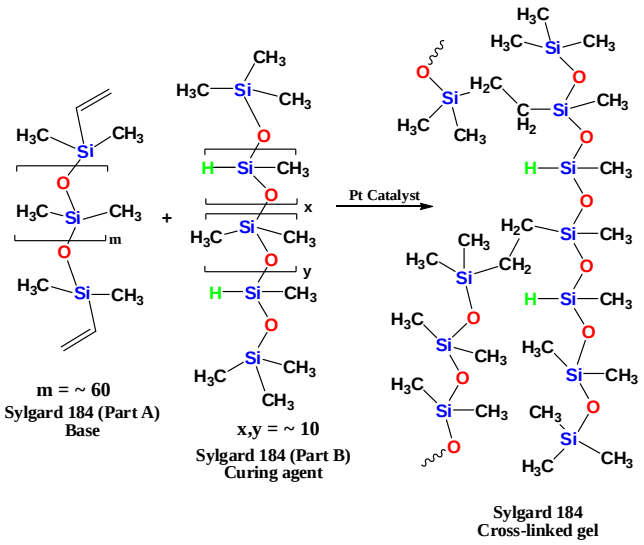

Figure 1 *The chemical structure of Sylgard®184 elastometers* [31]

Grassie's group [33] and others [34–38] have reported on thermal decomposition of linear chain PDMS in which each silicon is di-substituted $[(CH_3)_2Si\text{-}O]_n$ (D units). Pyrolysis of linear dimethylpolysiloxane does not yield char or any other type of infusible residue [33] due to complete depolymerization by evolution of a spectrum of cyclic compounds ranging from D_3-D_{12} units. Only very few studies have been reported on the thermal stability of PDMS Sylgard gel into SiC_xO_y ceramics. Cui *et al.* [39] described very briefly the thermogravimetry of Sylgard gel. The gel showed around 57% weight loss at 900 °C in nitrogen. The objective of this study is thus to evaluate the effect of curing agent content and pyrolysis conditions on the ceramic yield, and also the thermal stability of derived ceramics in oxidizing atmosphere.

2. Experimental

The starting polymers were prepared using commercially available Sylgard®184 elastomer. The curing agent and base were mixed in a given ratio of curing agent: base expressed in part by volume (PBV), and stirred thoroughly in a clean beaker.

The air bubbles and solvents were degassed in a vacuum chamber. The sol was transferred to a polystyrene dish, and allowed to cross-link at room temperature for a minimum of 60 h. The gels in square sizes 1.5 ×1.5 cm^2 were pyrolysed in an alumina horizontal tube furnace at a heating rate of 2 °C/min in a flow of 50 sccm (standard cubic centimeters per minute) of Argon (99.999%) purity.

The pyrolysis process was characterized using a thermobalance (Netzsch STA449 F1 apparatus) coupled with mass spectrometer (Netzsch QMS403D Aeolos, 1-300 amu, 70eV, electronic ionization). The volatile species evolved during the pyrolysis were transported to the mass spectrometer via a heated SiO_2 capillary of diameter 0.75 µm. The analysis was performed in a flowing argon atmosphere of 50 sccm, and with a heating rate of 10 °C/min. The oxidation of pyrolysed residues was conducted at the heating rate of 10 °C/min in 20%O_2 in Helium with a flow of 50 sccm.

A micro-Raman spectrometer (Horiba, Jobin-Yvon LabRam®HR) was used to record Raman spectra of the samples. A solid-state laser (Cobalt Blues® DPSS) having a wavelength of 473 nm focused on the sample using 100× objective lens. Raman scattered signal were collected, spectrally dispersed by a grating (1800 lines/mm) and then detected by a position sensitive CCD detector.

3. Results and discussion

3.1 Thermal conversion

A preliminary observation, already made by P.Vallet in his book [40], is that a TGA thermogram is useful and can be compared only when all experimental conditions are known precisely. Unfortunately, the few experiments performed on commercial Sylgard 184 precursors reported in literature cannot be used for comparison [30,39]. Many important factors (amount of material, heating rate, the nature of the carrier gas) that may affect decomposition behavior cannot be ignored and must be taken into account when comparing data.

For comparison, two different inert carrier gases (helium and argon) are used to sweep evolved gases out of the furnace to the mass spectrometer for volatile species analysis. To eliminate possible effects of sample mass on decomposition temperature, similar amounts of sample (40 mg) were placed into in the 160 mm diameter by 200 mm tall cylindrical alumina crucible and heated under the same conditions (heating rate 10 °C/min, carrier gas flow 50 sccm). The TG curves in Figure 2a of cross-linked gels in helium and in argon show similar patterns.

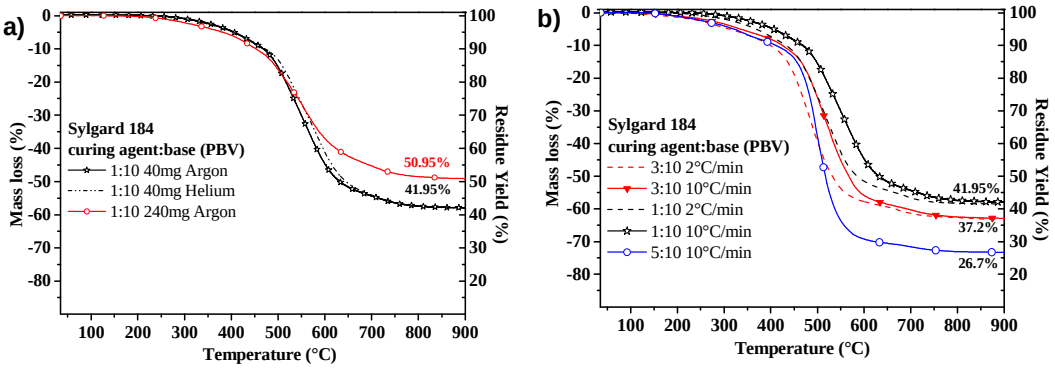

Figure 2 *Thermogravimetry analysis of cross-linked PDMS gels: (a) The effect of the nature of carrier gas (helium, argon), (b) influence of the heating rate on thermal degradation of gels*

For the gels prepared using 1:10 and 3:10 PBV (Part By Volume), the pyrolysis was conducted in argon atmosphere at two different heating rates (2 °C/min and 10

°C/min). As shown in Figure 2b, the TG profiles are nearly the same, only a slight shift in the temperature of the maximum mass loss is observed. Whatever the ratio of curing agent to base, increasing heating rate shifts the onset temperature to higher values, and subsequent mass loss occurs between 400 °C and 600 °C. For the gels prepared using the same ratio, the ceramic yield at 900 °C are found to be the same.

It can be seen that the mass loss of the gel is influenced by the volume % of the curing agent. Even though the mass loss profiles are the same, the main difference lies in the ceramic yield at 900 °C. The gels with 1:10 PBV result in the highest ceramic yield of 41.95%, whereas increasing the curing agent to 5:10 PBV decreases the ceramic yield to 26.7%, as shown in Figure 2. By comparison, it seems that the judicious amount of curing agent (1:10 PBV) impedes degradation and therefore increases the ceramic yield of PDMS. This is not surprising, since the gels containing D^H units (O-Si(HCH_3)-O are known to undergo thermal degradation around 400 °C to yield volatile products containing silicon [41]. As a result, the char yield markedly decreases.

It is also clear from the graph that there is a very discernible change when the initial mass of gel is varied from 40 mg to 250 mg. As the yield is the primary interest for design and fabrication of ceramic parts, the gel 1:10 PBV showing the highest yield of 41.95% has been selected for further analysis. The gaseous decomposition species were swept from the furnace toward the ionization chamber of the mass spectrometer. Figure 3 shows thermogravimetry-coupled with mass spectrometry (TG/MS) analysis of the cross-linked Sylgard®184 gel (1:10 PBV, 40 mg) at a heating rate of 10 °C/min in flowing helium atmosphere. Due to the presence of numerous different fragments, to provide a clear picture of the mass spectrometry (MS) profile curves, only ions of most importance to our discussion have been selected, and shown in Figure 3.

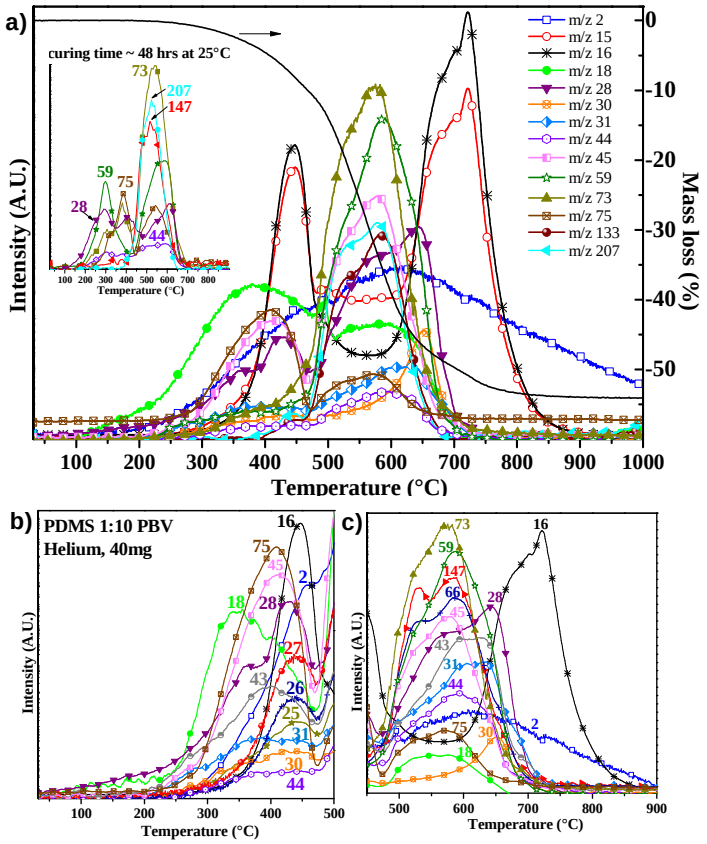

Figure 3 (a) *Thermogravimetry-coupled with mass spectrometry analysis of Sylgard®184 crosslinked polydimethylsiloxane elastometer in flowing Helium atmosphere, and magnified version in two temperature ranges (b) 30 °C – 500 °C and (c) 450 °C – 900 °C*

On heating from room temperature to 400 °C, the cross-linked gel exhibits a mass loss of ~ 4.61% to 18.5% depending on the concentration of curing agent. The gases detected correspond to hydrogen (m/z 2), water (m/z 18), and silicon-based species, mainly $(CH_3)_3$-Si-OH (m/z 75, 45, 47, 29, 43), and traces of $(CH_3)_3$-SiH (m/z 59, 73, 43, 58) ascribed to terminal sites of the curing agent (Figure 1). The presence of H_2O leads to the hydrolysis of $(CH_3)_3Si$-O- sites and to the cleavage of $(CH_3)_3Si$-OH (m/z 75, 45), as observed for Polyhydridomethyl siloxane PHMS $(CH_3SiHO)n$[41].

The extent of the mass loss depends on many factors such as the ratio of curing agent to base, the curing time, and the curing temperature of the gels. The gels prepared using curing agent to base ratio of 1:10 PBV and cured for ~ 48h at room temperature, show greater mass loss when compared to those cured during few months. This difference is due to the release of end sites which produces compounds of the type $(CH_3)_3SiH$ (m/z 59, 73), $(CH_3)_2SiH_2$ (m/z 59, 44, 28), as shown in the inset of Figure 3a. The more unreacted O-H bonds present in the gel, the greater the loss of end sites is.

The loss of water (m/z 18), and hydrogen (m/z 2) at this stage is associated with dehydration between two Si-OH [19], and dehydrocoupling reactions between Si-H and Si-OH respectively [19]. It should be noted that during the curing step via hydrosilylation reaction, the Pt catalyst also performs as a sluggish dehydrocoupling, slightly converting Si-H bonds to Si-OH due to the presence of moisture in the reaction solution.

Between 400 °C and 480 °C, the second weight loss of ~ 6.87% indicated the removal of hydrocarbon species such as methane CH_4 (m/z 16, 15, 14, 12), and ethylene C_2H_4 (m/z 28, 27, 26, 25). These species are issued from the vinyl terminal sites of PDMS-base, and to decomposition of $Si\text{-}C_2H_3$, as already shown on other organosiloxane polymers issued from $C_2H_3\text{-}SiO_{1.5}$ precursors[42,43].

A maximum mass loss of ~ 33.6 % has occurred in a temperature interval, ranging from 480 °C to 600 °C. Detected in this domain is a series of silicon-based oligomers such as linear molecules $(CH_3)_3\text{-}Si\text{-}O\text{-}Si\text{-}(CH_3)_3$ (m/z 147, 73, 66), and cyclic molecules such as $[(CH_3)_2\text{-}SiO]_3$, D_3 (m/z 207, 96, 191, 133) and $[(CH_3)_2\text{-}SiO]_5$, or D_5 (m/z 73, 355, 267, 45, 59), together with elimination of hydrogen (m/z 2) and water (m/z 18).

The thermal degradation proceeds via reactions, in which the main chain Si-O bonds undergo splitting and reformation. As shown in Figure 4, the exchange reactions of the siloxane readily occur within a single polymer or between two different macromolecules (intermolecular chains) [44]. The formation of cyclic volatiles extends from low molecular weight units such as D_3, D_4, D_5 to higher degrees of polymerization [33]. The formation of cyclic oligomers were explained by backbiting or unzipping mechanism due to presence of Si-OH groups (Figure 4a) or due to random scission (Figure 4b) [45].

It might be useful to recall that silicon-based oligomers can in turn undergo degradation reactions upon heating in the furnace and release volatile species.

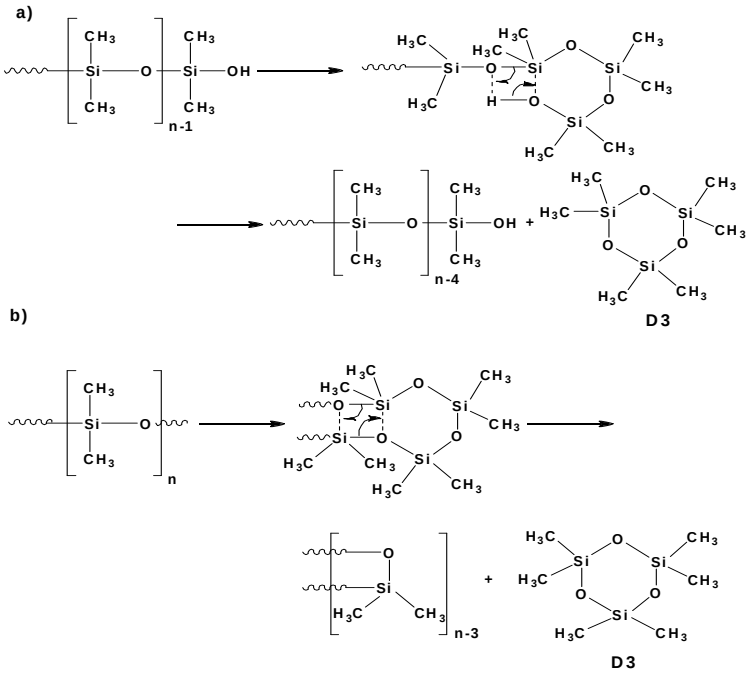

Figure 4 *Formation of cyclic oligomers D_3 units via (a) unzipping mechanism in presence of Si-OH, (b) random scission mechanism along the intramolecular siloxane backbone* [45].

In the temperature range 600 °C – 780 °C, predominant release of H_2 and CH_4 leads to a weight loss of ~ 12.4 %. In the presence of Si-H, the cleavage of Si-CH_3

occurs via free radical mechanisms [19]. It is noteworthy to mention that the free radical mechanisms via Si-H started earlier than the homolytic cleavage of Si-CH_3 which is peaked at 800 °C in the absence of Si-H, for example as for MTES [21]. All these reactions are well documented in the literature[19,44]

Further heating between 900 °C and 1500 °C, no significant mass loss was observed. However, annealing at 1500 °C, the material undergoes a further mass loss to produce mainly carbon monoxide CO (m/z 28, 12), as shown in Figure 5 via carbothermal reduction reactions [46].

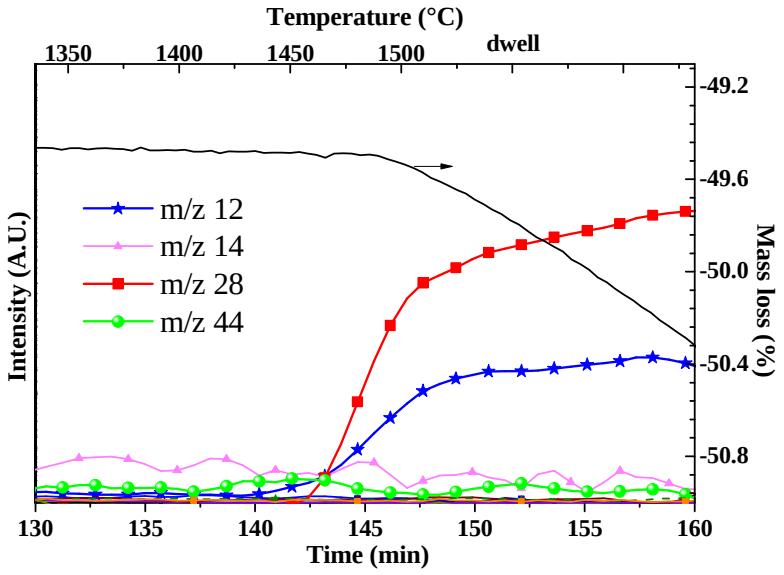

Figure 5 *Thermogravimetry-coupled with mass spectrometry analysis of Sylgard PDMS (1:10 PBV) at 1500 °C in inert atmosphere*

3.2 Raman spectroscopy analysis

Figure 6a depicts the Raman spectra recorded from Sylgard base (Part A), curing agent (Part B), and the 1:10 PVB cross-linked gel. By Raman spectroscopy, no significant differences were found between the freshly prepared and aged gels. In all three compounds, the most intense peaks appeared at 2907 cm^{-1} and 2965 cm^{-1} are

assigned to symmetric and asymmetric stretching vibration of CH in Si-CH_3 units, respectively.

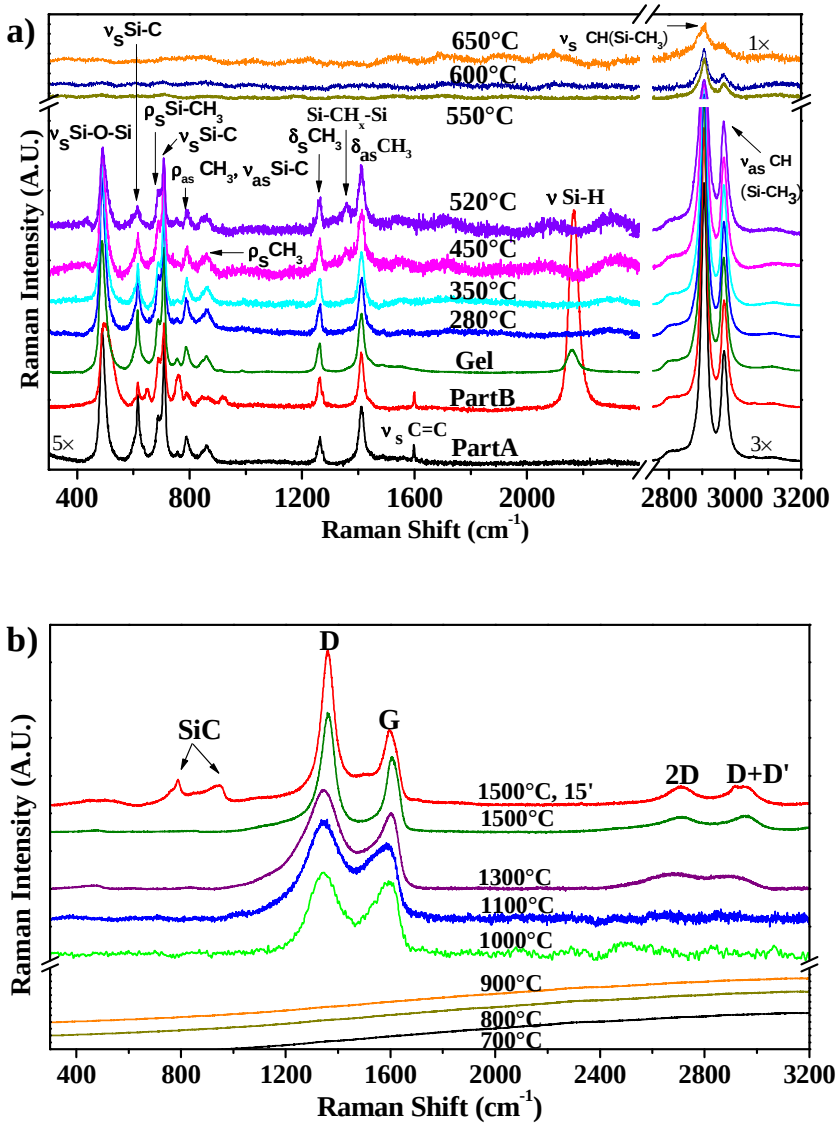

Figure 6 *Raman spectroscopy acquired from (a) PDMS Sylgard 184 base (part A), curing agent (part B), 1:10 PVB cross-linked gel, and heat treated up to 650 °C (b) ceramic residues issued from pyrolysis of 1:10 PVB cross-linked gel*

. A major difference between the base and cross-linking agent is noticeable at 2160 cm^{-1} that belongs to stretching vibration of Si-H. The only evidence signature for the presence of vinyl groups is the small signal near 1610 cm^{-1} (ν_s C=C). This could be

due either to their low concentration because vinyl groups have been converted by hydrosilylation or polyaddition reactions. This is observed for both parts (A and B) [31]. This shows that the curing agent is not pure; it may contain few percentages of dimethylsiloxane dimethylvinyl-terminated molecules, and tetramethyl tetravinyl cyclotetrasiloxane [32]. Note that in both parts of commercial PDMS-based products, the precise chemical composition and the nature of chemical structural are not known. The band at 488 cm^{-1} is characteristic of symmetric stretching of Si-O-Si. In the cross-linking agent, the band at 488 cm^{-1} is broad is broad relative to the base, which suggests that the environment of Si-O-Si in the cross-linker is different than the base.

The cross-linked gel features a weak and broad band at 2160 cm^{-1} indicating the presence of unreacted Si-H. The bands at 1412 cm^{-1}, 1262 cm^{-1}, and 862 cm^{-1} are attributed to asymmetric bending (δ_{as}), symmetric bending (δ_s) and symmetric rocking (ρ_s) of CH_3 group attached to silicon atom, respectively. The gel shows other weak bands at 708 cm^{-1} and 687 cm^{-1} assigned to symmetric stretching (ν_s), and rocking (ρ_s) of Si-C bonds. The band at 787 cm^{-1} was assigned to asymmetric rocking (ρ_{as}) vibration of CH_3 and/or asymmetric stretching (ν_{as}) of Si-C [47].

For comparison, the spectra acquired from the gel and those pyrolyzed up to 600 °C, were normalized with respect to the most intense peak at 2907 cm^{-1}. With increasing pyrolysis temperature up to 280 °C, the peak at 2160 cm^{-1} completely disappeared at 280 °C. This indicates that either all Si-H bonds have been consumed or that their content is too low to be detected by Raman spectroscopy. The sample heated between 350 °C and 520 °C exhibits a new peak at 1348 cm^{-1}. This peak was assigned to aliphatic chains CH_2-CH_2 between two silicon atoms [19], providing further evidence for the consumption of Si-H by hydrosilylation reaction between Si-H and Si-Vinyl bonds [41]. The overall intensity of all peaks gradually decreases with increasing heat

treatment temperatures (up to 650 °C). However, Si-CH_3 groups (2800-3000 cm^{-1}) persist to at least 650 °C. This agrees with the results obtained from mass spectrometry analysis showing that above 600 °C the main evolved gas is CH_4 arising from Si-CH_3 scission.

For the samples heated between 700 °C and 900 °C, the Raman spectrum is featureless due to overlap of the fluorescence background that makes difficult to resolve Raman signal. A reason for emission of the high intensity of fluorescence is the presence of hydrogen saturated non-radiative recombination centers [48]. In other words, appearance of fluorescence is a consequence of the presence of -CH bonds in the derived residues [49]. Indeed, the presence of hydrogen in the material is reinforced by the evolving H_2 gas detected by mass spectrometry when further heating the gel. Above 1000 °C, the characteristic bands of sp^2 disordered carbon appear even though fluorescence is still present. The two bands, namely graphitic (G) band centered around 1600 cm^{-1} and disorder induced (D) band at 1365 cm^{-1}, are attributed to the free carbon phase having turbostratic structure [50], in which a few layers of graphene are stacked randomly to each other. The G band is a result of in-plane vibrations of all pairs of sp^2 carbon either chains or rings, whereas the D band is associated to breathing mode of aromatic rings [51]. The D band is forbidden in perfect graphite, but it appears for disordered carbon structures. Both the G and D bands appear as a broad massif [52], which is an overlap of multiple defect bands namely D' (~ 1620 cm^{-1}), D'' (~ 1500 cm^{-1}), and T (~ 1200 cm^{-1}) bands [53,54]. For comparison, the spectra have been normalized with respect to the G band intensity in Figure 6b. The fitting procedure of the first order spectra was carried out using a set of Voigt function for both D and G bands, and a Gaussian function for the band centered at 1540 cm^{-1} that is assigned to sp^2 bonded carbons linked to heteroatoms, especially oxygen [55]. The intensity of the D

band increased with heat treatment temperature. Monthioux *et al.* [56] showed by TEM analysis that the C_{free} phase of most polymer-derived ceramics exists as basic structural units (BSU) of diameter lower than 0.7 nm.

Other peak characteristics, such as full width at half maximum (FHWM), and the positions of the D and G bands provide structural information of the free carbon phase [57]. For the samples heat-treated between 1000 °C and 1500 °C, the FWHM of D-band decreased from 152 cm^{-1} to 60 cm^{-1}, and that of G band decreased from 65.5 cm^{-1} to 58.3 cm^{-1}. These results suggest the occurrence of clustering of free carbon phase as the treatment temperature rises [52]. From known literature, the resulting black residues are composed of several mixed phases (SiC_xO_y) well described by solid NMR for the same type of materials derived from pyrolysis of hybrid organic-inorganic polymers [58],[20]. These black glasses are structurally heterogeneous systems containing excess free carbon. The ^{29}Si NMR analysis revealed various silicon environments; $SiCO_3$, SiC_2O_2, SiC_3O, SiC_4, and SiO_4. On further heating, the mixed structural phases undergo rearrangements yielding the most stable condensed phases such as SiO_2, SiC, and free carbon phases.

Indeed, after 1500 °C heat treatment for 15 min, the sample exhibited the characteristic peaks of SiC phase at 789 cm^{-1} and 916 cm^{-1}, as shown in Figure 6b. The formation of SiC is attributed to carbothermal reactions involving the mixed metastable phases SiC_xO_y, or SiO_4 sites and free carbon phase, according to equation (1) – (3) [43],[20].

$$SiC_xO_y \text{ -----> } SiC_{(s)} + x\,CO + (y-x-1)C \qquad (1)$$

$$SiO_2 + 3C \text{ ---> } SiO_{(g)} + 2CO_{(g)} \qquad (2)$$

$$SiO_{(g)} + 2C \text{ --->} SiC_{(s)} + CO_{(g)} \qquad (3)$$

All these reactions involving free carbon phase lead to a mass loss accompanied by a release of CO gas clearly shown by TG/MS (Figure 5), and as a consequence, a new organization of free carbon network occured.

3.3 Oxidation behavior of derived ceramics

In a first instance the oxidation behavior of pyrolyzed materials was tested in the TGA apparatus in a flowing mixture of oxygen and helium (20 % O_2 in He). The thermogravimetry analysis (Figure 7) clearly demonstrated that oxidation behavior of PDMS-derived materials depends on pyrolysis temperature. Among the three pyrolyzed samples, the one previously heated at the lowest temperature (1000 °C) exhibits a mass loss, whereas a slight variation in mass gain (0.35%) is found for samples pyrolyzed above 1000 °C.

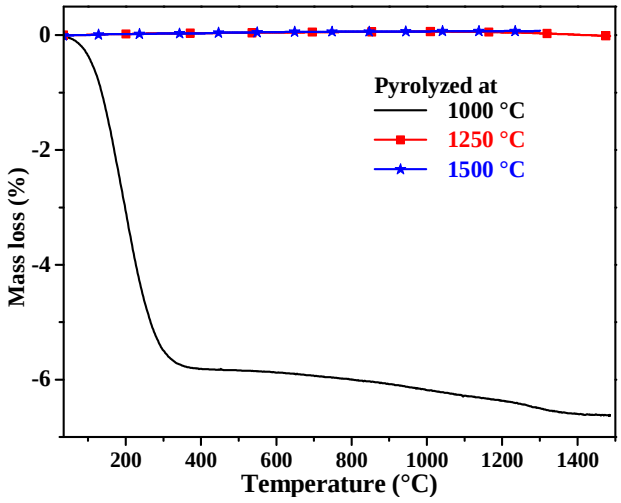

Figure 7 *Thermogravimetry analysis of polydimethylsiloxane (Sylgard184)-derived ceramics in oxidizing atmosphere*

It is well known that the oxidation of carbon-enriched oxycarbide materials involves several elementary reactions shown by equations 4 to 10 [59,60]. These reactions can occur either in parallel or in a series of sequential reactions. Some of these reactions lead to mass loss (equations 5, 6, 7, 8, 10), whereas others produce mass gain

(equations 4 and 9). It is worth noting that the reactions at the interface, as for example equation 9, given off SiO that will rapidly react to produce SiO_2 in the presence of oxygen. TG gives the resultant variation of mass, only.

$$–CH_2 + O_2 \rightarrow -C=O + H_2O \quad (4)$$

$$–C\text{-}H + O_2 \rightarrow CO_2 + H_2O \quad (5)$$

$$C_{free} + O_2 \rightarrow CO_2 \quad (6)$$

$$C_{free} + CO_2 \rightarrow 2CO \quad (7)$$

$$SiC_xO_y + O_2 \rightarrow SiO_2 + (CO, CO_2) \quad (8)$$

$$SiC + SiO_2 \text{ (at the interface in inner material)} \rightarrow 2SiO + C \quad (9)$$

$$3C + SiO_2 \text{ (at the interface in inner material)} \rightarrow SiC + 2CO \quad (10)$$

To better define the existence of several mixed phases present in the material, the Temperature Programmed Oxidation (TPO) of PDMS-derived ceramic materials has been achieved using TG coupled with MS analysis. The TPO procedure allow us to follow, simultaneously, the uptake of oxygen from mixed gas (20%O_2/Helium) by the sample, as well as the gases released during the oxidation reactions. Figure 8 illustrates the TG-MS data generated from oxidation of the sample previously pyrolyzed at 1500 °C.

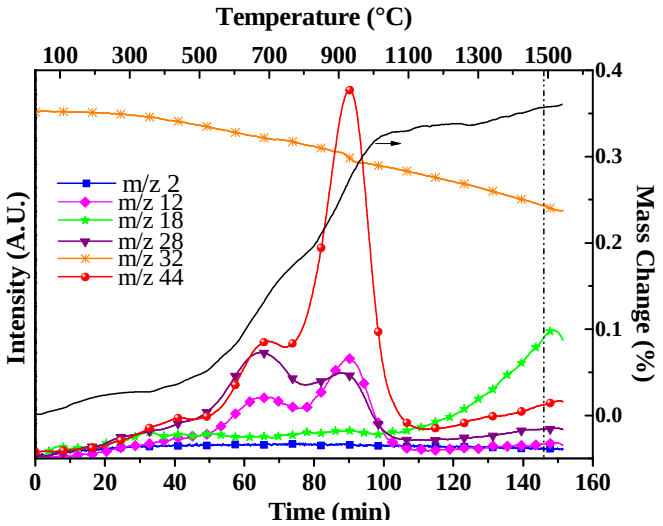

Figure 8 *Thermogravimetry coupled with mass spectrometry conducted at 10 °C/min in oxidizing atmosphere of PDMS previously pyrolyzed at 1500 °C*

The material is not sensitive to hydrolysis and has shown excellent oxidation behavior over a wide range of temperatures (25 °C - 1500 °C). Only, a very small gain in weight of ~ 0.35% is observed. Under linear heating, the main oxidation products detected were CO_2 (m/z 44, 28, 12), CO (m/z 28, 12) and also H_2O (m/z 18, 17). It is interesting to note that the TPO profile of CO_2 showed a series of peaks; one clear peak at 932 °C with several shoulders (at 439 °C, 686 °C, and at higher temperatures ~1500 °C). Each peak represents a distinct reactivity corresponding to a particular chemical environment site.

One of the most significant advantages of the method is its sensitivity to the structural features of phases involved in oxidation reactions. However, further studies by solid NMR and chemical analysis are required to better understand the chronological order of the reactivity of the various SiC_xO_y sites.

The mass gain seems more related with the oxidation of at least four different environments of silicon ($Si_xC_yO_z$). It can be noted that the carbon, present in the 1500 °C product, appears to be embedded in a continuous silicon oxycarbide phase and is not

easily oxidized due to the formation of a protective silica layer that inhibits further diffusion of oxygen. After oxidation, the structure of sp^2 carbon domains was revealed by Raman spectroscopy as shown in Figure 9.

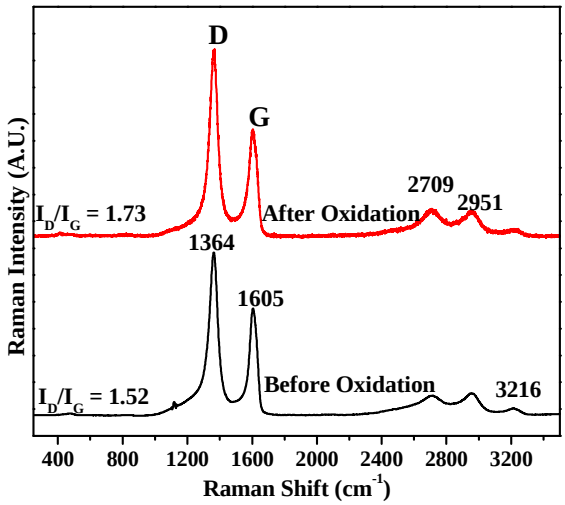

Figure 9 Comparison of the *Raman spectra acquired from PDMS-derived materials pyrolyzed at 1500 °C before and after oxidation at 1500 °C*

The Raman spectra of the samples pyrolyzed at 1500 °C, before and after oxidation at 1500 °C, are shown in Figure.9. Whatever the gaseous atmosphere of thermal treatment, heating at 1500 °C facilitates the arrangement of sp^2 carbon domains. After oxidation, no significant changes were detected in the characteristic positions of the two D and G-bands. Free carbon phase persists even after oxidizing treatment at 1500 °C. However, the I_D/I_G ratio increased from 1.52 to 1.73. The increasing and narrowing of the D band in the oxidized sample are clear evidence of an ordering of the sp^2 carbons leading to a better structural organization of free carbon phase. It is worthy to mention that our Raman experiments were performed at a laser power of 1 μW in order to avoid any local heating effects that can modify the characteristic of the two bands [61].

4. Conclusion

To date, little has been reported on the thermal conversion of commercially available PDMS-Sylgard®184. The present work encompasses the preparation of cured-PDMS gels, their thermal degradation, the structural characterization of resulting materials at different stages of pyrolysis, and finally their thermal resistance in oxidizing atmosphere.

The crosslinked polydimethylsiloxane gel (Sylgard®184) undergoes physical and structural changes when heated in an inert atmosphere. During the course of pyrolysis, a large weight loss (49%) occurred between 150 °C and 600 °C due to the cleavage of chemical bonds and depolymerization of siloxane units as trimers or higher degree cyclic oligomers. These reactions are very common in pyrolysis of organosiloxane polymers. The thermal degradation leaves a solid ceramic residue consisting of free carbon phase embedded into a silicon oxycarbide matrix. Raman spectroscopy showed the presence of the two characteristic bands (D and G) of disordered graphitic carbon in the residues.

Increasing pyrolysis temperature facilitates the removal of heteroatoms and dangling bonds surrounding carbon cycles and therefore favoring neighbouring carbon cycles to lie and also the rearrangement and orientation of carbon planes to take place. Thus, the diameter in plane (L_a) of the free carbon phase increases with further increase of pyrolysis temperature.

When pyrolyzed samples are subjected to oxidation, the mass variation depends on the treatment temperature of pyrolysis. The samples pyrolyzed above 1250 °C are remarkably resistant to oxidation and retains almost their initial mass due to the formation of SiO_2 layer at the surface of material. The SiO_2 layer acts as a protective

layer that prevents the oxygen diffusion. Therefore, carbon clusters are momently protected against oxygen attack.

Polymeric derived materials approach may be considered as an elegant method for producing composites in which nanometric carbon phase is well dispersed into an oxide matrix. Compared to traditional mixing or melting methods to produce composites, there is no need to handle the individual phases or to mix them in a liquid dispersion medium.

Preliminary results already published [23] have demonstrated the ability of PDMS to form near net-shaped structures, and the possibility to vary terahertz absorption coefficients of materials by changing the heat treating process.

The combination of these properties makes carbon-rich silicon oxycarbide materials derived from hybrid organic-inorganic polymers promising candidates for absorbers or also as black-body for terahertz thermal sources that can be used in hash environments.

References

[1] S. Yajima, J. Hayashi, M. Omori, Continuous silicon carbide fiber of high tensile strength, Chemistry Letters. 4 (1975) 931–934.

[2] J. Hayashi, K. Okamura, S. Yajima, Structural analysis in continous silicon carbide fiber of high tensile strength, Chemistry Letters. 4 (1975) 1209–1212.

[3] S. Yajima, Y. Hasegawa, J. Hayashi, M. Iimura, Synthesis of continuous silicon carbide fibre with high tensile strength and high Young's modulus, Journal of Materials Science. 13 (1978) 2569–2576. doi:10.1007/bf02402743.

[4] F.S. Kipping, The Bakerian Lecture. Organic Derivatives of Silicon, Proceedings of the Royal Society of London. Series A - Mathematical and Physical Sciences. 159 (1937) 139–148. doi:10.1098/rspa.1937.0063.

[5] F.S. Kipping, L.L. Lloyd, XLVII.-Organic derivatives of silicon. Triphenylsilicol and alkyloxysilicon chlorides, Journal of the Chemical Society, Transactions. 79 (1901) 449–459. doi:10.1039/ct9017900449.

[6] O. Flores, R.K. Bordia, D. Nestler, W. Krenkel, G. Motz, Ceramic Fibers Based on SiC and SiCN Systems: Current Research, Development, and Commercial Status, Advanced Engineering Materials. 16 (2014) 621–636. doi:10.1002/adem.201400069.

[7] L. David, R. Bhandavat, U. Barrera, G. Singh, Silicon oxycarbide glass-graphene composite paper electrode for long-cycle lithium-ion batteries, Nature Communications. 7 (2016) 10998. doi:10.1038/ncomms10998.

[8] S. Mukherjee, Z. Ren, G. Singh, Molecular polymer-derived ceramics for applications in electrochemical energy storage devices, J. Phys. D: Appl. Phys. 51 (2018) 463001. doi:10.1088/1361-6463/aadb18.

[9] Z.C. Eckel, C. Zhou, J.H. Martin, A.J. Jacobsen, W.B. Carter, T.A. Schaedler, Additive manufacturing of polymer-derived ceramics, Science. 351 (2016) 58–62. doi:10.1126/science.aad2688.

[10] E. Zanchetta, M. Cattaldo, G. Franchin, M. Schwentenwein, J. Homa, G. Brusatin, P. Colombo, Stereolithography of SiOC Ceramic Microcomponents, Advanced Materials. 28 (2016) 370–376. doi:10.1002/adma.201503470.

[11] P. Colombo, J.R. Hellmann, D.L. Shelleman, Mechanical Properties of Silicon Oxycarbide Ceramic Foams, Journal of the American Ceramic Society. 84 (2001) 2245–2251. doi:10.1111/j.1151-2916.2001.tb00996.x.

[12] F. Kolar, V. Machovic, J. SVitilova, L. Borecka, Structural characterization and thermal oxidation resistance of silicon oxycarbides produced by polysiloxane pyrolysis, Materials Chemistry and Physics. 86 (2004) 88–98. doi:10.1016/j.matchemphys.2004.02.011.

[13] J. Kaspar, M. Graczyk-Zajac, R. Riedel, Carbon-rich SiOC anodes for lithium-ion batteries: Part II. Role of thermal cross-linking, Solid State Ionics. 225 (2012) 527–531. doi:10.1016/j.ssi.2012.01.026.

[14] F. Roth, O. Guillon, E. Ionescu, N. Nicoloso, C. Schmerbauch, R. Riedel, Piezoresistive Ceramics for High-Temperature Force and Pressure Sensing, in: Sensors and Measuring Systems 2014; 17. ITG/GMA Symposium; Proceedings Of, 2014: pp. 1–4.

[15] S. Gallis, V. Nikas, H. Suhag, M. Huang, A.E. Kaloyeros, White light emission from amorphous silicon oxycarbide (a-SiCxOy) thin films: Role of composition and postdeposition annealing, Applied Physics Letters. 97 (2010) 081905. doi:10.1063/1.3482938.

[16] A. Karakuscu, R. Guider, L. Pavesi, G.D. Sorarù, White Luminescence from Sol–Gel-Derived SiOC Thin Films, Journal of the American Ceramic Society. 92 (2009) 2969–2974. doi:10.1111/j.1551-2916.2009.03343.x.

[17] W. Duan, X. Yin, Q. Li, L. Schlier, P. Greil, N. Travitzky, A review of absorption properties in silicon-based polymer derived ceramics, Journal of the European Ceramic Society. (2016). doi:10.1016/j.jeurceramsoc.2016.02.002.

[18] S. Venkatachalam, G. Ducournau, J.F. Lampin, D. Hourlier, Synthesis of carbon-based composites and their intrinsic properties in sub-millimeter wave domain, in: Journées de Caractérisation Microondes et Matériaux, 2016.

[19] D. Bahloul-Hourlier, J. Latournerie, P. Dempsey, Reaction pathways during the thermal conversion of polysiloxane precursors into oxycarbide ceramics, Journal of the European Ceramic Society. 25 (2005) 979–985. doi:10.1016/j.jeurceramsoc.2004.05.012.

[20] P.H. Mutin, Control of the Composition and Structure of Silicon Oxycarbide and Oxynitride Glasses Derived from Polysiloxane Precursors, Journal of Sol-Gel Science and Technology. 14 (1999) 27–38. doi:10.1023/a:1008769913083.

[21] J. Latournerie, Ceramiques nanocomposites SiCO : Synthese, caracterisation et stabiblite thermique, Unversite de Limoges, 2002.

[22] P. Colombo, G. Mera, R. Riedel, G.D. Sorarù, Polymer-Derived Ceramics: 40 Years of Research and Innovation in Advanced Ceramics, Journal of the American Ceramic Society. 93 (2010) 1805–1837. doi:10.1111/j.1551-2916.2010.03876.x.

[23] S. Venkatachalam, G. Ducournau, J.-F. Lampin, D. Hourlier, Net-shaped pyramidal carbon-based ceramic materials designed for terahertz absorbers, Materials & Design. 120 (2017) 1–9.

[24] S. Martinez-Crespiera, E. Ionescu, M. Schlosser, K. Flittner, G. Mistura, R. Riedel, H.F. Schlaak, Fabrication of silicon oxycarbide-based microcomponents via photolithographic and soft lithography approaches, Sensors and Actuators A: Physical. 169 (2011) 242–249. doi:10.1016/j.sna.2011.04.041.

[25] X. Liu, Y.-L. Li, F. Hou, Fabrication of SiOC Ceramic Microparts and Patterned Structures from Polysiloxanes via Liquid Cast and Pyrolysis, Journal of the American Ceramic Society. 92 (2009) 49–53. doi:10.1111/j.1551-2916.2008.02849.x.

[26] J. Grossenbacher, M.R. Gullo, R. Grandjean, T. Kiefer, J. Brugger, Sub micrometer ceramic structures fabricated by molding a polymer-derived ceramic, Microelectronic Engineering. 97 (2012) 272–275. doi:10.1016/j.mee.2012.04.024.

[27] B. He, N.A. Patankar, J. Lee, Multiple Equilibrium Droplet Shapes and Design Criterion for Rough Hydrophobic Surfaces, Langmuir. 19 (2003) 4999–5003. doi:10.1021/la0268348.

[28] R. Sivakumarasamy, K. Nishiguchi, A. Fujiwara, D. Vuillaume, N. Clement, A simple and inexpensive technique for PDMS/silicon chip alignment with sub-[small mu]m precision, Analytical Methods. 6 (2014) 97–101. doi:10.1039/c3ay41618f.

[29] A. Folch, M. Toner, Cellular Micropatterns on Biocompatible Materials, Biotechnology Progress. 14 (1998) 388–392. doi:10.1021/bp980037b.

[30] R.T. Johnson, R.M. Biefeld, J.A. Sayre, High-temperature electrical conductivity and thermal decomposition of Sylgard® 184 and mixtures containing hollow microspherical fillers, Polymer Engineering & Science. 24 (1984) 435–441. doi:10.1002/pen.760240608.

[31] G.C. Lisensky, D.J. Campbell, K.J. Beckman, C.E. Calderon, P.W. Doolan, M.O. Rebecca, A.B. Ellis, Replication and Compression of Surface Structures with Polydimethylsiloxane Elastomer, Journal of Chemical Education. 76 (1999) 537. doi:10.1021/ed076p537.

[32] D. Ortiz-Acosta, Sylgard (R) Cure Inhibition characterization, Los Alamos National Labatory, USA, 2012.

[33] N. Grassie, I.G. Macfarlane, The thermal degradation of polysiloxanes: I. Poly(dimethylsiloxane), European Polymer Journal. 14 (1978) 875–884. doi:10.1016/0014-3057(78)90084-8.

[34] T.H. Thomas, T.C. Kendrick, Thermal analysis of polydimethylsiloxanes. I. Thermal degradation in controlled atmospheres, Journal of Polymer Science Part A-2: Polymer Physics. 7 (1969) 537–549. doi:10.1002/pol.1969.160070308.

[35] T.H. Thomas, T.C. Kendrick, Thermal analysis of polysiloxanes. II. Thermal vacuum degradation of polysiloxanes with different substituents on silicon and in the main siloxane chain, Journal of Polymer Science Part A-2: Polymer Physics. 8 (1970) 1823–1830. doi:10.1002/pol.1970.160081016.

[36] D.J. Bannister, J.A. Semlyen, Studies of cyclic and linear poly(dimethyl siloxanes): 6. Effect of heat, Polymer. 22 (1981) 377–381. doi:10.1016/0032-3861(81)90050-1.

[37] G. Camino, S.M. Lomakin, M. Lazzari, Polydimethylsiloxane thermal degradation Part 1. Kinetic aspects, Polymer. 42 (2001) 2395–2402. doi:10.1016/S0032-3861(00)00652-2.

[38] S.J. Clarson, J.A. Semlyen, Studies of cyclic and linear poly (dimethyl-siloxanes): 21. High temperature thermal behaviour, Polymer. 27 (1986) 91–95.

[39] M. Cui, W. Wang, Thermal properties study on the ablation materials of inorganic silicon compound from organosilicone in high percent conversion, Chinese Science Bulletin. 52 (2007) 2048–2053. doi:10.1007/s11434-007-0313-y.

[40] P. Vallet, Thermogravimétrie : étude critique et théorique: utilisation, principaux usages, Gauthier-Villars, 1972. https://books.google.fr/books?id=dJN2OwAACAAJ.

[41] D. Hourlier, S. Venkatachalam, M.-R. Ammar, Y. Blum, Pyrolytic conversion of organopolysiloxanes, Journal of Analytical and Applied Pyrolysis. (n.d.). doi:10.1016/j.jaap.2016.11.016.

[42] D. R. Bujalski, S. Grigoras, W. Lee, G. M. Wieber, G. A. Zank, Stoichiometry control of SiOC ceramics by siloxane polymer functionality, Journal of Materials Chemistry. 8 (1998) 1427–1433. doi:10.1039/a800708j.

[43] J. Latournerie, P. Dempsey, D. Hourlier-Bahloul, J.-P. Bonnet, Silicon Oxycarbide Glasses: Part 1—Thermochemical Stability, Journal of the American Ceramic Society. 89 (2006) 1485–1491. doi:10.1111/j.1551-2916.2005.00869.x.

[44] P.H. Mutin, Role of Redistribution Reactions in the Polymer Route to Silicon–Carbon–Oxygen Ceramics, Journal of the American Ceramic Society. 85 (2002) 1185–1189. doi:10.1111/j.1151-2916.2002.tb00243.x.

[45] R. Jones, W. Ando, J. Chojnowski, Silicon-Containing Polymers, 1st ed., Springer Netherlands, 2000.

[46] A.W. Weimer, K.J. Nilsen, G.A. Cochran, R.P. Roach, Kinetics of carbothermal reduction synthesis of beta silicon carbide, AIChE Journal. 39 (1993) 493–503. doi:10.1002/aic.690390311.

[47] S.C. Bae, H. Lee, Z. Lin, S. Granick, Chemical Imaging in a Surface Forces Apparatus: Confocal Raman Spectroscopy of Confined Poly(dimethylsiloxane), Langmuir. 21 (2005) 5685–5688. doi:10.1021/la050233+.

[48] C. Casiraghi, A.C. Ferrari, J. Robertson, Raman spectroscopy of hydrogenated amorphous carbons, Physical Review B. 72 (2005) 085401.

[49] F. Dalcanale, J. Grossenbacher, G. Blugan, M.R. Gullo, A. Lauria, J. Brugger, H. Tevaearai, T. Graule, M. Niederberger, J. Kuebler, Influence of carbon enrichment on electrical conductivity and processing of polycarbosilane derived ceramic for MEMS applications, Journal of the European Ceramic Society. 34 (2014) 3559–3570. doi:10.1016/j.jeurceramsoc.2014.06.002.

[50] A. Oberlin, Carbonization and graphitization, Carbon. 22 (1984) 521–541. doi:10.1016/0008-6223(84)90086-1.

[51] A.C. Ferrari, J. Robertson, Raman spectroscopy of amorphous, nanostructured, diamond-like carbon, and nanodiamond, Philosophical Transactions of the Royal Society of London A: Mathematical, Physical and Engineering Sciences. 362 (2004) 2477–2512. doi:10.1098/rsta.2004.1452.

[52] D. Deldicque, J.-N. Rouzaud, B. Velde, A Raman-HRTEM study of the carbonization of wood: A new Raman-based paleothermometer dedicated to archaeometry, Carbon. 102 (2016) 319–329. doi:10.1016/j.carbon.2016.02.042.

[53] A. Cuesta, P. Dhamelincourt, J. Laureyns, A. Martinez-Alonso, J.M.D. Tascon, Raman microprobe studies on carbon materials, Carbon. 32 (1994) 1523–1532. doi:10.1016/0008-6223(94)90148-1.

[54] G. Mera, A. Navrotsky, S. Sen, H.-J. Kleebe, R. Riedel, Polymer-derived SiCN and SiOC ceramics - structure and energetics at the nanoscale, Journal of Materials Chemistry A. 1 (2013) 3826–3836. doi:10.1039/c2ta00727d.

[55] S. Karlin, P. Colomban, Raman Study of the Chemical and Thermal Degradation of As-Received and Sol–Gel Embedded Nicalon and Hi-Nicalon SiC Fibres Used in Ceramic Matrix Composites, Journal of Raman Spectroscopy. 28 (1997) 219–228. doi:10.1002/(sici)1097-4555(199704)28:4<219::aid-jrs88>3.0.co;2-f.

[56] M. Monthioux, O. Delverdier, Thermal behavior of (organosilicon) polymer-derived ceramics. V: Main facts and trends, Journal of the European Ceramic Society. 16 (1996) 721–737. doi:10.1016/0955-2219(95)00186-7.

[57] M. Inagaki, N. Ohta, Y. Hishiyama, Aromatic polyimides as carbon precursors, Carbon. 61 (2013) 1–21. doi:10.1016/j.carbon.2013.05.035.

[58] V. Gualandris, D. Hourlier-Bahloul, F. Babonneau, Structural Investigation of the First Stages of Pyrolysis of Si-C-O Preceramic Polymers Containing Si-H Bonds, Journal of Sol-Gel Science and Technology. 14 (1999) 39–48. doi:10.1023/a:1008771729921.

[59] R.R. Naslain, Ceramic matrix composites, Phil. Trans. R. Soc. Lond. A. 351 (1995) 485–496. doi:10.1098/rsta.1995.0048.

[60] C.M. Brewer, D.R. Bujalski, V.E. Parent, K. Su, G.A. Zank, Insights into the Oxidation Chemistry of SiOC Ceramics Derived from Silsesquioxanes, Journal of Sol-Gel Science and Technology. 14 (1999) 49–68. doi:10.1023/a:1008723813991.

[61] M.J. Matthews, M.A. Pimenta, G. Dresselhaus, M.S. Dresselhaus, M. Endo, Origin of dispersive effects of the Raman D band in carbon materials, Phys. Rev. B. 59 (1999) R6585–R6588. doi:10.1103/PhysRevB.59.R6585.